

The Biologically Important Surfactin Lipopeptide Induces Nanoripples in Supported Lipid Bilayers

Robert Brasseur,[†] Nathalie Braun,[‡] Karim El Kirat,[‡] Magali Deleu,[§]
Marie-Paule Mingeot-Leclercq,^{||} and Yves F. Dufrêne^{*‡}

Centre de Biophysique Moléculaire Numérique, Faculté Universitaire des Sciences Agronomiques de Gembloux, Passage des Déportés 2, B-5030 Gembloux, Belgium, Unité de Chimie des Interfaces, Université Catholique de Louvain, Croix du Sud 2/18, B-1348 Louvain-la-Neuve, Belgium, Unité de Chimie Biologique Industrielle, Faculté Universitaire des Sciences Agronomiques de Gembloux, Passage des Déportés 2, B-5030 Gembloux, Belgium, and Unité de Pharmacologie Cellulaire et Moléculaire, Université Catholique de Louvain, UCL 73.70, Avenue E. Mounier 73, B-1200 Brussels, Belgium

Received May 21, 2007. In Final Form: June 25, 2007

Under specific conditions, lipid membranes form ripple phases with intriguing nanoscale undulations. Here, we show using in situ atomic force microscopy (AFM) that the biologically important surfactin lipopeptide induces nanoripples of 30 nm periodicity in dipalmitoyl phosphatidylcholine (DPPC) bilayers at 25° (i.e. well below the pretransition temperature of DPPC). Whereas most undulations formed the classical straight orientation with characteristic angle changes of 120°, some of them also displayed unusual circular orientations. Strikingly, ripple structures were formed at 15% surfactin but were rarely or never observed at 5 and 30% surfactin, emphasizing the important role played by the surfactin concentration. Theoretical simulations corroborated the AFM data by revealing the formation of stable surfactin/lipid assemblies with positive curvature.

Introduction

Surfactins are surface-active lipopeptides produced by *Bacillus subtilis* strains composed of a cyclic heptapeptide on which a fatty acid chain is branched (Figure 1).¹ They are attracting more and more attention because of their high surface activity^{2,3} and their remarkable biological properties including antiviral and antibacterial activity.^{4,5} Because the biological activity of surfactin relies directly on its interaction with membranes, understanding the molecular interactions, mixing behavior, and domain formation of this lipopeptide within lipid bilayers is an important challenge.

Depending on temperature and lipid composition, lipid bilayers can form different phases. A striking example is the ripple phase, which is observed only for certain lipids such as phosphatidylcholines (PC), in a temperature range between the pretransition temperature and the main phase-transition temperature. A remarkable feature of this phase is the formation of corrugations with periods in the range of 10 to 30 nm depending on the lipid nature.^{6,7} In PC bilayers, two different ripple structures form—a stable one and a metastable one—depending on the thermal history

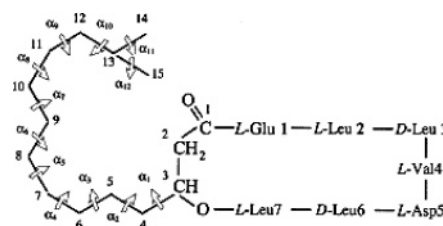


Figure 1. Primary structure of surfactin showing the numbering of the carbon atoms of the β -hydroxy fatty acid side chain and the torsional angles.

of the sample. The stable ripple phase (denoted $\Lambda/2$) has a ripple repeat distance of ~ 15 nm and forms at the pretransition temperature upon heating from the gel phase whereas the metastable ripple phase (denoted Λ) forms at the main phase transition upon cooling from the fluid phase and has an ~ 30 nm repeat distance.^{8,9} Several factors have been proposed to account for the local spontaneous curvature of the lipid bilayer, including electrostatic coupling between water molecules and the polar lipid headgroups, coupling between lipid membrane curvature and molecular tilt, and the generation of curvature by linear arrays of fluid-state lipid molecules.^{6–9} Yet, the mechanisms and biological roles of ripple-phase formation remain poorly understood at the molecular level.

During the past decade, atomic force microscopy (AFM) has been increasingly used to explore the structure of biological specimens,^{10,11} including supported lipid bilayers.^{12–22} Owing

* Corresponding author. E-mail: dufrêne@cifa.ucl.ac.be. Phone: (32) 10 47 36 00. Fax: (32) 10 47 20 05.

[†] Centre de Biophysique Moléculaire Numérique, Faculté Universitaire des Sciences Agronomiques de Gembloux.

[‡] Unité de Chimie des Interfaces, Université Catholique de Louvain.

[§] Unité de Chimie Biologique Industrielle, Faculté Universitaire des Sciences Agronomiques de Gembloux.

^{||} Unité de Pharmacologie Cellulaire et Moléculaire, Université Catholique de Louvain.

(1) Kakinuma, A.; Ouchida, A.; Shima, T.; Sugino, H.; Isono, M.; Tamura, G.; Arima, K. *Agric. Biol. Chem.* **1969**, *33*, 1669.

(2) Maget-Dana, R.; Ptak, M. *J. Colloid Interface Sci.* **1992**, *153*, 285.

(3) Razafindralambo, H.; Thonart, P.; Paquot, M. *J. Surfactants Deterg.* **2004**, *7*, 41.

(4) Vollenbroich, D.; Özel, M.; Vater, J.; Kamp, R. M.; Pauli, G. *Biologicals* **1997**, *25*, 289.

(5) Vollenbroich, D.; Pauli, G.; Özel, M.; Vater, J. *Appl. Environ. Microbiol.* **1997**, *63*, 44.

(6) Nagle, J. F.; Tristram-Nagle, S. *Biochim. Biophys. Acta* **2000**, *1469*, 159.

(7) Heimburg, T. *Biophys. J.* **2000**, *78*, 1154.

(8) Leidy, C.; Kaasgaard, T.; Crowe, J. H.; Mouritsen, O. G.; Jorgensen, K. *Biophys. J.* **2002**, *83*, 2625.

(9) Kaasgaard, T.; Leidy, C.; Crowe, J. H.; Mouritsen, O. G.; Jorgensen, K. *Biophys. J.* **2003**, *85*, 350.

(10) Engel, A.; Müller, D. *J. Nat. Struct. Biol.* **2000**, *7*, 715.

(11) Jena, B. P.; Hörber, J. K. H., Eds. *Atomic Force Microscopy in Cell Biology*; Methods in Cell Biology; Academic Press: San Diego, CA, 2002; Vol. 68.

(12) Mou, J. X.; Yang, J.; Shao, Z. F. *Biochemistry* **1994**, *33*, 4439.

(13) Mou, J. X.; Czajkowsky, D. M.; Shao, Z. F. *Biochemistry* **1996**, *35*, 3222.

(14) Czajkowsky, D. M.; Huang, C.; Shao, Z. F. *Biochemistry* **1995**, *34*, 12501.

(15) Fang, Y.; Yang, J. *J. Phys. Chem.* **1996**, *100*, 15614.

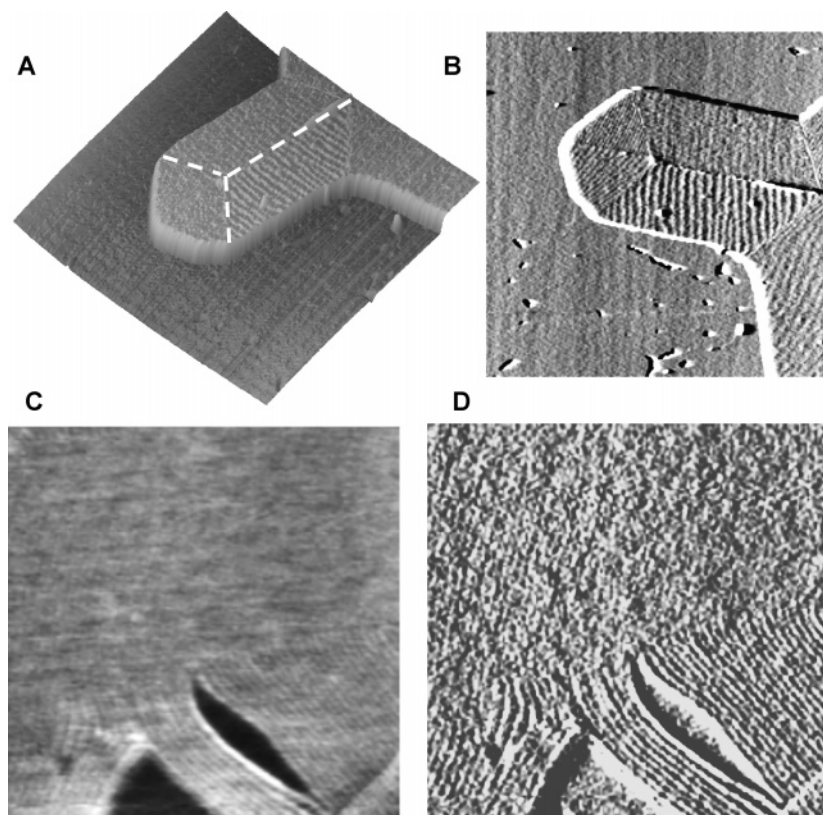


Figure 2. AFM height (A, C) and deflection (B, D) images (A, B: $5 \mu\text{m} \times 5 \mu\text{m}$; C, D: $1.5 \mu\text{m} \times 1.5 \mu\text{m}$; z scales: 25 and 5 nm for A and C, respectively) of mixed surfactin/DPPC (0.15, 0.85) bilayers. Dashed lines in A show changes in ripple direction with a characteristic angle of 120° .

to its nanoscale lateral resolution and ability to work in liquid, AFM has allowed researchers to visualize ripple phases in supported lipid bilayers.^{8,9,12–15} However, the formation of a ripple phase triggered by lipopeptides has never been reported. Here, we used AFM to demonstrate that surfactin induces the formation of nanoripples in dipalmitoylphosphatidylcholine (DPPC) bilayers at 25° (i.e., well below the pretransition temperature of DPPC (32°C)). In light of theoretical simulations, we suggest a mechanism by which the local curvature of bilayer undulations is promoted by the conical shape of surfactin assemblies.

Materials and Methods

Dipalmitoylphosphatidylcholine (1,2-dihexadecanoyl-*sn*-glycero-3-phosphocholine) (DPPC) was purchased from Sigma (St. Louis, MO), and surfactin was produced by *B. subtilis* S499. The primary structure and purity of the surfactin (>95%) were ascertained by analytical RP-HPLC (Vydack $10 \mu\text{m}$ C18 column, $0.46 \times 25 \text{ cm}^2$, Vydack, Hesperia, CA), amino acid analysis, and MALDI-TOF mass spectrometry measurements (Ultraflex TOF, Bruker, Karlsruhe, Germany). The surfactin mixture was 95.4% pure and was mainly composed of surfactin-C13, surfactin-C14, and surfactin-C15 (0.3/1/1).

Surfactin and DPPC were dissolved separately in chloroform to 6 mM final concentration. Mixtures of surfactin/DPPC containing

5, 15, and 30 mol % lipopeptide were prepared and evaporated under nitrogen and then dried in a desiccator under vacuum for 2 h. Multilamellar vesicles (MLV) were obtained by resuspending the dried film in calcium-containing buffer (10 mM Tris, 150 mM NaCl, 3 mM CaCl_2 , pH 8.5) to 1.2 mM final concentration. To obtain small unilamellar vesicles (SUV), the suspension was sonicated to clarity (three cycles of 2.5 min) using a 500 W probe sonicator (Fisher Bioblock Scientific, France; 35% of the maximal power; 13 mm probe diameter) while keeping the suspension in an ice bath. The liposomal suspension was then filtered on $0.2 \mu\text{m}$ nylon filters (Whatman Inc.) to eliminate titanium particles.

Supported lipid bilayers were prepared using the vesicle fusion method.²² Briefly, $150 \mu\text{L}$ of the SUV suspension was applied to freshly cleaved mica (16 mm^2). Vesicles were allowed to adsorb on mica overnight at 4°C . After rinsing with 3 mL of buffer (10 mM Tris, 150 mM NaCl, pH 8.5) at 4°C , the samples were heated to 60°C for 60 min and then left to cool slowly to room temperature. The obtained bilayers were never allowed to dry in order to avoid membrane reorganization and further defect formation.

Supported bilayers were investigated using a commercial AFM (NanoScope IV MultiMode AFM, Veeco Metrology LLC, Santa Barbara, CA) equipped with a $12 \mu\text{m} \times 12 \mu\text{m}$ scanner (E-scanner). AFM images were obtained in contact mode at room temperature ($23\text{--}25^\circ\text{C}$) in Tris buffer (10 mM Tris, 150 mM NaCl, pH 8.5). All images were recorded using oxide-sharpened microfabricated Si_3N_4 cantilevers (Microlevers, Veeco Metrology LLC, Santa Barbara, CA) with a spring constant of 0.01 N/m (manufacturer specified) using a minimal applied force (<500 pN) and a scan rate of 5 to 6 Hz.

The hypermatrix in silico procedure was used to calculate surfactin complexes from isolated surfactin molecules on the basis of energy minimization. This procedure has already been used to analyze molecule interactions for a series of molecules, the most recent being the interaction of a CRAC motif and cholesterol.^{23,24} By this procedure, two molecules of surfactin, one named the central molecule and the other named the moving molecule, are positioned at a

(16) Dufrène, Y. F.; Barger, W. R.; Green, J. B. D.; Lee, G. U. *Langmuir* **1997**, *13*, 4779–4784.

(17) Dufrène, Y. F.; Lee, G. U. *Biochim. Biophys. Acta* **2000**, *1509*, 14–41.

(18) Rinia, H. A.; Kik, R. A.; Demel, R. A.; Snel, M. M. E.; Killian, J. A.; van der Eerden, J. P. J. M.; de Kruijff, B. *Biochemistry* **2000**, *39*, 5852.

(19) Janshoff, A.; Steinem, C. *ChemBioChem* **2001**, *2*, 798–808.

(20) Giocondi, M.-C.; Vié, V.; Lesniewska, E.; Milhiet, P.-E.; Zinke-Allmang, M.; Le Grimmelc, C. *Langmuir* **2001**, *17*, 1653.

(21) Reviakine, I.; Bergsma-Schutter, W.; Morozov, A. N.; Brisson, A. *Langmuir* **2001**, *17*, 1680.

(22) Rinia, H. A.; Boots, J. W.; Rijkers, D. T.; Kik, R. A.; Snel, M. M.; Demel, R. A.; Killian, J. A.; van der Eerden, J. P.; de Kruijff, B. *Biochemistry* **2002**, *41*, 2814.

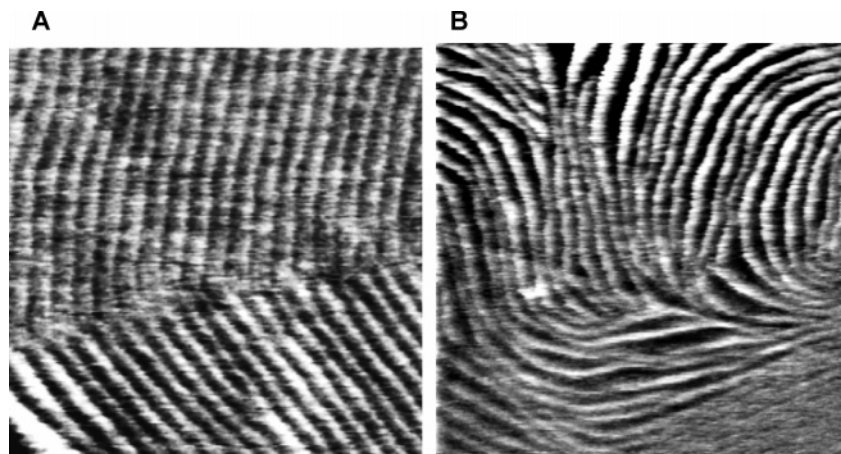


Figure 3. High-resolution height images (A: $600 \text{ nm} \times 600 \text{ nm}$; B: $1 \mu\text{m} \times 1 \mu\text{m}$; z scales: 2 nm) of mixed surfactin/DPPC (0.15, 0.85) bilayers. Whereas most ripple structures show straight orientations that change in direction with a 120° angle (A), some structures displayed unusual circular orientations (B).

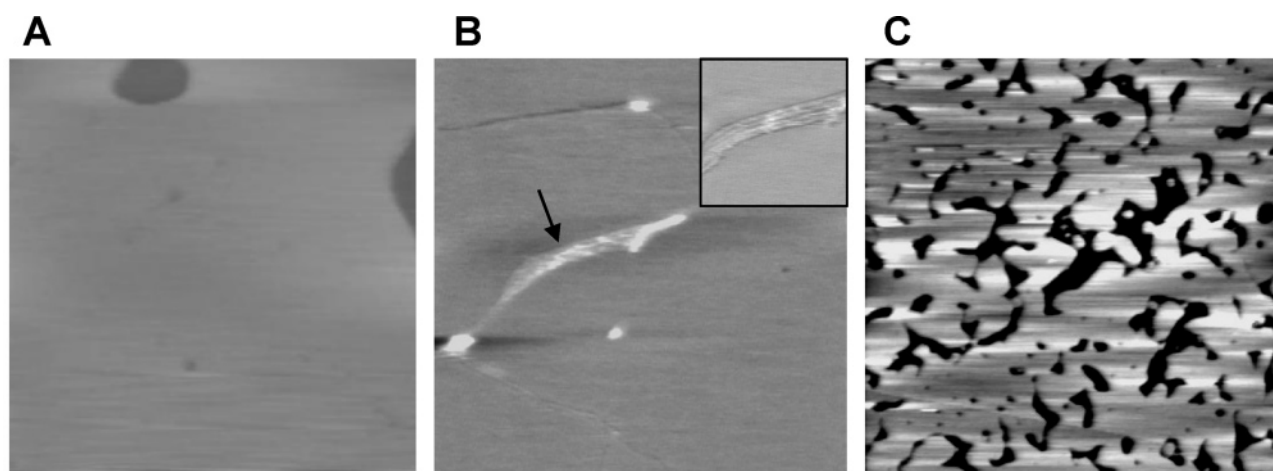


Figure 4. Height images (A, B: $3 \mu\text{m} \times 3 \mu\text{m}$; C: $5 \mu\text{m} \times 5 \mu\text{m}$; z scales: 5 nm) of DPPC bilayers containing 0 (A), 5 (B), and 30% (C) surfactin. The inset in B shows an enlarged view ($1 \mu\text{m} \times 1 \mu\text{m}$) of the corrugations highlighted by the arrow.

membrane interface in accordance with their 3D structure, apparent hydrophobicity, and membrane hydrophobicity gradient. Then, the energy of interaction of the central molecule with the moving molecule of surfactin is calculated for a large series (> 107) of relative positions. Varying parameters of the relative positions are translations of the moving molecule in the membrane plane and perpendicular to that plane, the tilt with respect to the central molecule axis, and the rotations of the moving molecule, with the latter movements being both self-rotation and rotation around the central molecule. The energy of interactions of the two surfactin molecules in all positions is stored in a hypermatrix of energy. Multimolecular associations of surfactin molecules are calculated by combining several solutions from the hypermatrix of interaction. The dimer is made up of the most stable complex. A trimer is made by adding to the dimer the next energetically stable position after checking for the absence of steric clash. This procedure is iterated for the trimer and subsequent molecules, up to when the addition of one more surfactin is no longer possible. The final solution is the complex.

Results and Discussion

Mixed DPPC/surfactin bilayers were prepared by vesicle fusion onto freshly cleaved mica and imaged in situ by AFM. Figure 2 shows AFM height and deflection images obtained at 25° for surfactin/DPPC (0.15 and 0.85 mol/mol) bilayers. Two discrete

levels were clearly observed, separated by a height difference of $7.4 \pm 0.3 \text{ nm}$ that corresponds to the DPPC bilayer thickness.⁸ Moreover, holes were frequently seen in the lower region (Figure 2B), indicating the presence of double bilayers supported on mica, the second bilayer only partially covering the first bilayer.

Notably, the second bilayer exhibited nanoscale undulations that are clearly reminiscent of a ripple phase. Although these structures were observed only on the second bilayer, it remains to be elucidated whether the first bilayers contain surfactin. Also visible were changes in the undulation direction by an angle of 120° , indicating hexagonal packing of the lipid chains. Although this behavior is characteristic of ripple orientations,⁹ it may also reflect other phenomena involving domain boundary formation in lipid bilayers (see, for example, work by Rinia and colleagues).¹⁸ At higher magnification (Figure 3A), cross-section analyses reveal an undulation periodicity of $30 \pm 2.5 \text{ nm}$, which is fully consistent with the characteristics of metastable ripple phases (Λ) forming upon cooling from the fluid phase.⁹ As can be seen in Figure 3B, some ripples did not show the classical straight orientation but formed circular shapes. Accordingly, the above data indicate that surfactin at 15% concentration induces the formation of ripple-like surface morphology in DPPC bilayers. Similar effects induced by Tris and gramicidin have been demonstrated in phosphatidylcholine bilayers.^{12,13}

To address the question as to whether the surfactin concentration modulates its ability to induce ripple structures, we imaged

(23) Brasseur, R.; Killian, J. A.; de Kruijff, B.; Ruyschaert, J. M. *Biochim. Biophys. Acta* **1987**, *903*, 11.

(24) Epand, R. F.; Thomas, A.; Brasseur, R.; Vishwanathan, S. A.; Hunter, E.; Epand, R. M. *Biochemistry* **2006**, *45*, 6105.

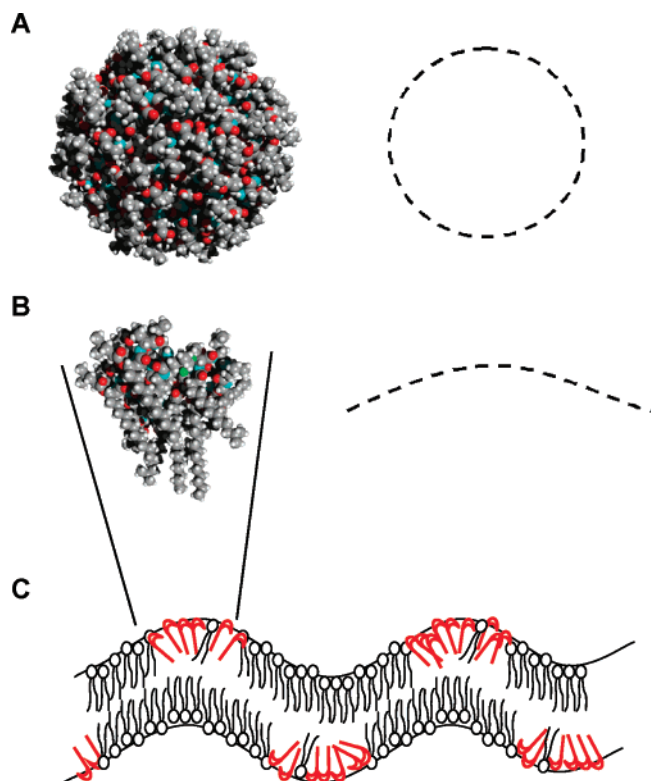


Figure 5. (A) Multimolecular assembly of 35 surfactin molecules generated by theoretical simulation, revealing the formation of a stable micellar organization; shown on the right is a schematic representation of the spherical micelle interface. (B) Mixed assembly of two DPPC and five surfactin molecules in interaction, indicating the formation of stable cone-shaped structures with less pronounced curvature. (C) Schematic drawing of a mixed surfactin/DPPC bilayer illustrating how cone-shaped surfactin assemblies (in red) may promote positive curvature in the bilayer by accumulating in the concave regions of the undulations, thereby favoring the ripple phase.

DPPC bilayers containing 0, 5, and 30% surfactin (Figure 4). In the absence of surfactin, ripple phases were never observed (Figure 4A), confirming that ripples are induced by the presence of surfactin. At 5% surfactin, corrugations were found, but only in very localized regions of the bilayers (Figure 4B), which may reflect the beginning of the large-scale ripples observed at 15% surfactin. By contrast, at 30% surfactin, the bilayers did not show any ripple structures and formed essentially single bilayers (Figure 4C). Furthermore, numerous large holes were observed in the bilayer, suggesting that high concentrations of surfactin lead to bilayer destabilization. Future work is needed to assess whether this behavior is related to a detergent effect, which is well known to occur with surfactin at high concentrations.^{4,5} These observations emphasize the important role played by surfactin concentration in inducing the ripple phase.

Next, we performed theoretical simulations to gain insight into the supramolecular structure of surfactin/lipid assemblies

(Figure 5). Calculations on pure surfactin assemblies revealed that they form a micellar organization in which peptide rings form the outer shell and fatty acid chains interact with each other to form the core of the micelle (Figure 5A). Interestingly, mixed surfactin/DPPC assemblies formed cone-shaped structures with much less pronounced positive curvature than pure surfactin assemblies (Figure 5B). Also, we note that the curvature was clearly anisotropic because it was observed only along specific orientations. This molecular model, which agrees well with our AFM images qualitatively, leads us to suggest the following mechanism to account for the ripple phase formation. Mixed surfactin/DPPC assemblies would promote anisotropic positive membrane curvature by accumulating in the concave regions of the bilayer undulations (Figure 5C), thereby stabilizing the ripple structures at temperatures smaller than the pretransition temperature. Hence, stable ripple structures would result from periodic variations of gel, DPPC-rich, and fluid surfactin-rich regions, which is fully consistent with earlier studies showing that DPPC and surfactin have a tendency to form gel and fluid domains in mixed films.^{4,5} Further simulations are necessary to provide more quantitative data on surfactin/lipid interactions and to answer the following questions: why are the ripple structures observed only at 15%, and why do they form undulations with 30 nm periodicity?

In conclusion, we have shown, using *in situ* AFM imaging, that 15% surfactin induces the formation of a ripple phase in DPPC bilayers at temperatures well below the pretransition temperature of DPPC. Whereas most undulations formed the classical straight orientation with a characteristic angle change of 120°, some undulations displayed very unusual circular orientations. Ripple structures were rarely observed at 5% and were never observed at 30% surfactin, emphasizing the important role played by the surfactin concentration. An important issue for future research is to perform more detailed studies in solution and on surfaces, using, for example, differential scanning calorimetry and attenuated total reflection Fourier transform infrared spectroscopy to gain further insight into surfactin–lipid interactions. Another exciting challenge would be to understand better the influence of the sample thermal history on ripple-phase formation using a temperature-controlled AFM.²⁰ For instance, pure DPPC bilayers could be imaged at room temperature, and following a subsequent addition of surfactin, the sample could be heated and cooled while being imaged.

Acknowledgment. This work was supported by the National Foundation for Scientific Research (FNRS), the Université Catholique de Louvain (Fonds Spéciaux de Recherche), the Federal Office for Scientific, Technical and Cultural Affairs (Interuniversity Poles of Attraction Programme), and the Région wallonne. Y.F.D. and M.D. are Research Associates of the FNRS, and R.B. is Research Director of the FNRS.

LA7014868